PROTEINS: Structure, Function, and Genetics 45:190–198 (2001)

New Insights into the Mechanism of Protein–Protein Association

Tzvia Selzer and Gideon Schreiber*
Department of Biological Chemistry, Weizmann Institute of Science, Rehovot, Israel

ABSTRACT **Association of a protein complex follows a two-step mechanism, with the first step being the formation of an encounter complex that evolves into the final complex. Here, we analyze recent experimental data of the association of TEM1-β-lactamase with BLIP using theoretical calculations and simulation. We show that the calculated Debye–Hückel energy of interaction for a pair of proteins during association resembles an energy funnel, with the final complex at the minima. All attraction is lost at inter-protein distances of 20 Å, or rotation angles of >60° from the orientation of the final complex. For faster-associating protein complexes, the energy funnel deepens and its volume increases. Mutations with the largest impact on association (hotspots for association) have the largest effect on the size and depth of the energy funnel. Analyzing existing evidence, we suggest that the transition state along the association pathway is the formation of the final complex from the encounter complex. Consequently, pairs of proteins forming an encounter complex will tend to dissociate more readily than to evolve into the final complex. Increasing directional diffusion by increasing favorable electrostatic attraction results in a faster forming and slower dissociating encounter complex. The possible applicability of electrostatic calculations for protein–protein docking is discussed. Proteins 2001;45:190–198.** © 2001 Wiley-Liss, Inc.

Key words: electrostatic rate enhancement; protein complexes; protein–protein interactions; protein association; protein engineering; simulation

INTRODUCTION

Specific, rapid interactions between proteins are fundamental for many processes in life. The association reaction begins by a random search of the two molecules for each other within the vast space of solution, followed by a precise docking of the two interfaces. The rate of the random search is dictated by Brownian motion, resulting in a rate constant of 7×10^9 $M^{-1}s^{-1}$, given by the Smolochowski–Einstein equation.[1] However, a random collision between two protein partners is far from ensuring complex formation, as their relative orientations dictate additional constraints, which slow down the rate of the reaction by three to five orders of magnitude.[2–4] This rate can be increased substantially by favorable long-range electrostatic forces.[2] The role of electrostatic attraction in the process of association of protein complexes was studied using Brownian dynamic simulations,[5–11] or by relating electrostatics to the average interaction potential between the active sites of two proteins.[12,13] Finally, a good quantitative relation between the electrostatic rate enhancement of protein complex formation and the electrostatic energy of interaction (ΔU) of a pair of proteins was demonstrated.[14]

The association of a pair of proteins can be described as a two-step reaction:

$$A + B \underset{k_{-1}}{\overset{k_1}{\rightleftharpoons}} A{:}B \underset{k_{-2}}{\overset{k_2}{\rightleftharpoons}} AB$$

where A and B are the free proteins, $A{:}B$ is the encounter complex, and AB is the final complex. According to this scheme, two proteins will diffuse randomly in solution until they reach an area, designated the steering region, where mutual electrostatic attraction leads them to the formation of a specific encounter complex. The nature of this encounter complex has been a matter of considerable research.[3,4,13,15–20] It is described as a low free energy attractor, i.e., a precursor state before docking, which is an ensemble of configurations whose average resembles the final complex. The encounter complex is stabilized by a combination of electrostatic forces and desolvation, and is destabilized by unfavorable entropy. Specific short-range interactions do not seem to play an important role at this stage.[15–17,19,20] The formation of the final complex from the encounter complex requires desolvation and structural rearrangement of the side chains, thus removing steric clashes and charge overlaps upon binding.

The association and dissociation pathways can be probed experimentally either by changing solution conditions or by site-directed mutagenesis. Extensive site directed mutagenesis studies have demonstrated that only mutations involving charged residues have a significant effect on measured values of k_{on} (Fig. 1). In contrast, mutations of uncharged resides are neutral with respect to k_{on}.[19,21] However, the magnitude Δk_{on} per Δ charge is not a fixed quality, but is specific for each mutant. The calculation of the rate of association from the electrostatic attraction

Grant sponsor: Crown Endowment.

*Correspondence to: Gideon Schreiber, Weizmann Institute of Science, Rehovot, 76100 Israel. E-mail: bcges@weizmann.ac.il

Received 4 April 2001; Accepted 14 May 2001

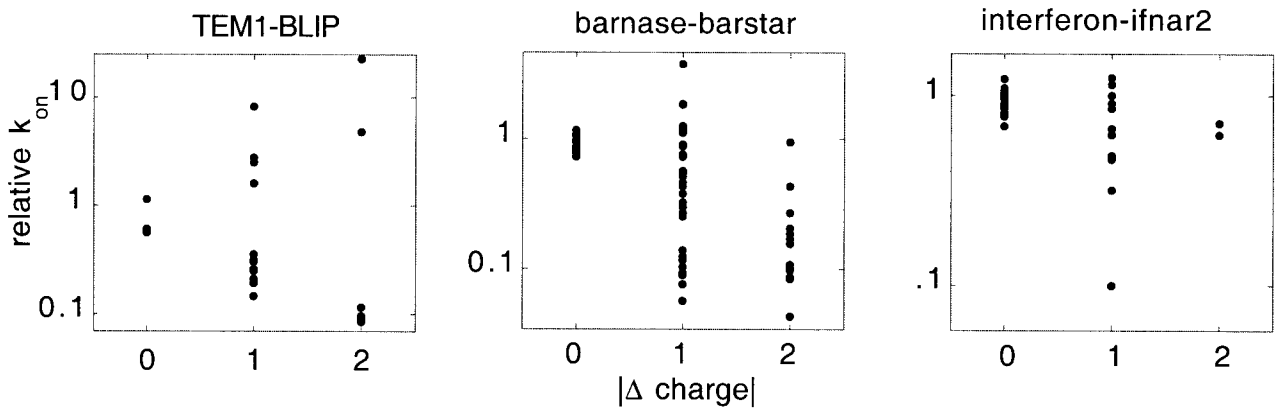

Fig. 1. Change in the rate of association caused by mutation (as determined experimentally) plotted versus the change in the absolute charge of the protein complex. Data from refs. 14, 21, 28, 30.

between two proteins (including the effect of screening of charges by salt) was made possible using the computer program PARE.[14] PARE calculates the k_{on} of protein complexes from the difference in the Debye–Hückel energy between the two individual proteins and their complex. Although a simplified set of parameters is used for calculations (all charges are immersed in a homogeneous dielectric constant of 80 with no boundary between the interior and exterior of the proteins), calculated values of k_{on} simulate the experimental data with a high degree of accuracy. We attribute this to three main reasons: (1) charges are located on the surface of proteins, (2) the difference between the Poisson–Boltzmann and Coulombic energies is very small once the proteins are separated by >5 Å[4] and (3) a nonlinear term was incorporated in the Debye–Hückel calculations $\frac{e^{-\kappa(r_{ij}-a)}}{1+\kappa a}$ ($a = 6\,\text{Å}$), which results in an increase in the calculated electrostatic energy between close residues and in a decrease in the calculated energy between distant residues. This seems to compensate for the homogeneous dielectric constant used. The applicability of this program has been recently highlighted by the success to increase the experimentally measured rate of association of TEM1-β-lactamase and its protein inhibitor BLIP by 250-fold.[14] This was done by altering the electrostatic potential of BLIP to be optimized to bind TEM1 rapidly via mutation of residues outside, albeit at the periphery of the binding site. This rate increase was predicted precisely by calculation with PARE, applying only electrostatic considerations. Using the same sets of parameters in PARE, the rates of association of about 40 selected mutations of barnase–barstar, acetylcholinesterase–fasciculin, and hirudin–thrombin, for which measured k_{on} values were available, were calculated. A correlation of 0.985 was determined between calculated and experimental data. Thus, it seems reasonable to investigate the association and dissociation reaction of a pair of proteins by analyzing the relationship between electrostatics and binding.

In this study, we combine an experimental and computational electrostatic analysis to obtain new insights into the association pathway. Following the principle of macromolecular reversibility, we consider both the association and dissociation pathways in the analysis. We show that the basic steps leading to protein–protein association include a step of random diffusion, followed by directional diffusion leading to the formation of an encounter complex. The encounter complex is very unstable and tends to dissociate more rapidly than to evolve into the bound complex. As the encounter complex is stabilized by long-range electrostatic forces, its tendency to evolve into the final complex rate increase caused by favorable long-range electrostatic forces is proportional to k_1k_2/k_{-1}, where k_1k_2 relates to the contribution of electrostatic forces to steering and k_{-1} relates to the stabilization of the encounter complex.

Most of the theoretical analysis in this article is performed on the association between TEM1-β-lactamase and BLIP. This system is especially suitable for this study, as different single and multiple TEM1–BLIP mutants are available which alter the rate of association in the range of 5,000-fold.[14,22] A major difficulty in attributing the effects of mutations toward a specific physical phenomena is that mutations propagate secondary changes on their environment. In the case presented, all mutations in BLIP were designed to be located outside the TEM1 binding site, so that they neither alter the structural integrity of the interface nor interfere with the final steps of association (precise docking and desolvation). Thus, the effects measured are a result of charge perturbation due to changes in the electrostatic potential of the system. As electrostatic forces act over large distances, these mutations had a significant effect on the rates of association, while the rates of dissociation were constant for all mutations analyzed.[14]

RESULTS AND DISCUSSION

Investigating the Nature of the Steering Region Using Simulation

Recently we described the ability of the computer program PARE to calculate accurately the rate of association of protein complexes, as well as its applicability to protein design. In the present article, we use PARE to follow the changes in the electrostatic energy of interaction between two pairs of proteins; TEM1 interacting with BLIP and

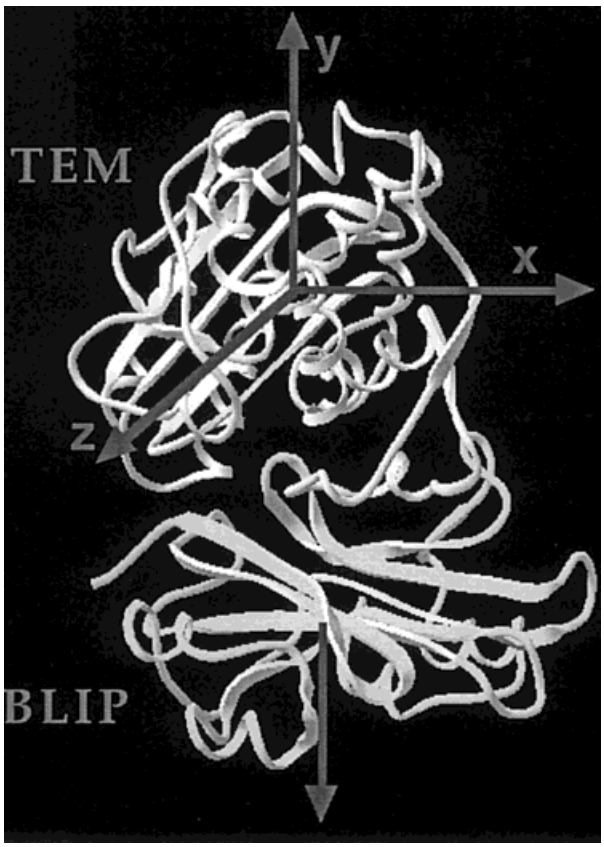

Fig. 2. Graphic representation of the TEM1–BLIP complex,[26] with *xyz* being the coordinate system for rotation, fixed to the TEM1 center of mass. Simulations of the PARE energy of interaction at different relative orientations and interprotein distances were done as follows. The interfacial plane between the interacting proteins was defined to lie in the *x*,*z*-plane. Starting with the final protein–protein complex BLIP was translated along the *y*-axes in 5 Å increments to a maximum distance of 25 Å. The coordinate file of the translated protein complex at each increment was recorded. At each incremental distance, BLIP was fixed, while TEM1 was rotated around its center of mass. Rotations were made around the three principal axes with increments of 30°, i.e., 34 rotational conformations (including the wt conformation) for each distance. The Debye–Hückel energy of interaction between the proteins was calculated at each distance (6 values) for all 34 conformations using PARE.[14] The coordinate files of the translated and rotated protein systems were generated using the pdbset/ccp4 package.[33] It is important to note that movements around the *y*-axis cause the smallest relative movements of interfacial residues, particularly for residues located close to the axis. All calculations were done at an ionic strength of 22 mM, at which experimental data were measured for all mutant proteins.

barnase with barstar as they approach each other. The magnitude of the Debye–Hückel energy of interaction (ΔU) was calculated at different relative orientations and at different distances separating the proteins. For TEM1–BLIP (Fig. 2), values of ΔU were calculated for the wild-type proteins and three BLIP mutants: (T140K + Q157K), D163K, and the (+6) mutant (V165K + D163K + D135K + N89K) (Fig. 3). The experimentally determined rates of association of these BLIP mutants associating with TEM1 are increased by a factor of 5, 23, and 250, respectively relatively to wild-type proteins.[14] The calculations show that at a distance of >25 Å (at I = 22 mM) values of ΔU are about zero, independent of the mutant analyzed, or the relative orientations of the proteins. Thus, electrostatic steering seems to play a role at relative short interprotein distances. In this work we define the electrostatic steering region as the region of the six-dimensional space where favorable electrostatic energy of interaction between the two proteins is larger than k_BT, and is progressively increasing toward the final complex. For the wild-type interaction between TEM1 and BLIP, the proteins enter the steering region only near the final complex [Fig. 3(a)]. In contrast, for the faster associating BLIP mutants: (T140K + Q157K), D163K, and (+6), $\Delta U = k_BT$ is reached at a distance of about 5, 10, and 20 Å, respectively [Fig. 3(b–d)]. Thus, the size of the steering region increases for faster associating protein complexes. An alternative approach to visualize the steering region is illustrated in Figure 4. Here, the magnitude of the Debye–Hückel energy of interaction (ΔU) is plotted in 3D versus the distance and the relative rotation angle between the proteins. From the shallow wells, it is apparent that very little electrostatic guidance is observed for the wild-type complex [Fig. 4(a–c)], in line with our notion that the association of TEM1 and BLIP is not electrostatically driven. However, for the (+6) BLIP variant, which associates 250-fold faster than wild-type, the energy landscape resembles a funnel, with the final complex occupying the lowest electrostatic energy point [Fig. 4(d–f)]. This is independent of the rotation axis chosen. However, greater attraction is observed over longer distances only at the correct orientation. At relative rotations of >60°, all the attraction is lost; thus, a small rotation of one of the proteins is sufficient to exit the steering region. These results are in line with the experimental observation that the size of the steering region is increased with increasing electrostatic energy of interaction.[23] Aside from the increased size of the steering region for the faster associating proteins, the absolute values of ΔU increase as well. This has important implications toward the stabilization of the encounter complex, as discussed later. In Figure 5 the simulations done for TEM1–BLIP were repeated for the interaction of barnase with barstar, rotating barstar relative to barnase. The outcome is similar to that obtained for TEM1–BLIP. Both the *x* and *z*-axis rotations show electrostatic funneling [Fig. 5(a,c)], whereas ΔU is almost unaffected by rotating barstar around the *y*-axis. This is attributable to the homogeneous charge distribution in the barnase binding site on barstar, which occupies the *x*,*z*-plane and is dominated by six negative charges.[19,21,24]

General Mechanism for Association

Figure 6 illustrates two possible pathways for protein–protein association. The highest energy barrier along the reaction pathway [Fig. 6(a)] is the transition between the encounter complex and the final complex [AB]. In Figure 6(b), the highest energy barrier is located before the encounter complex [A:B], suggesting that once [*A*:*B*] is formed, it will evolve rapidly to form [*AB*]. In the following section, we demonstrate, in light of the above simulations and previous experimental results, that the pathway of association presented in Figure 6(a) describes to our

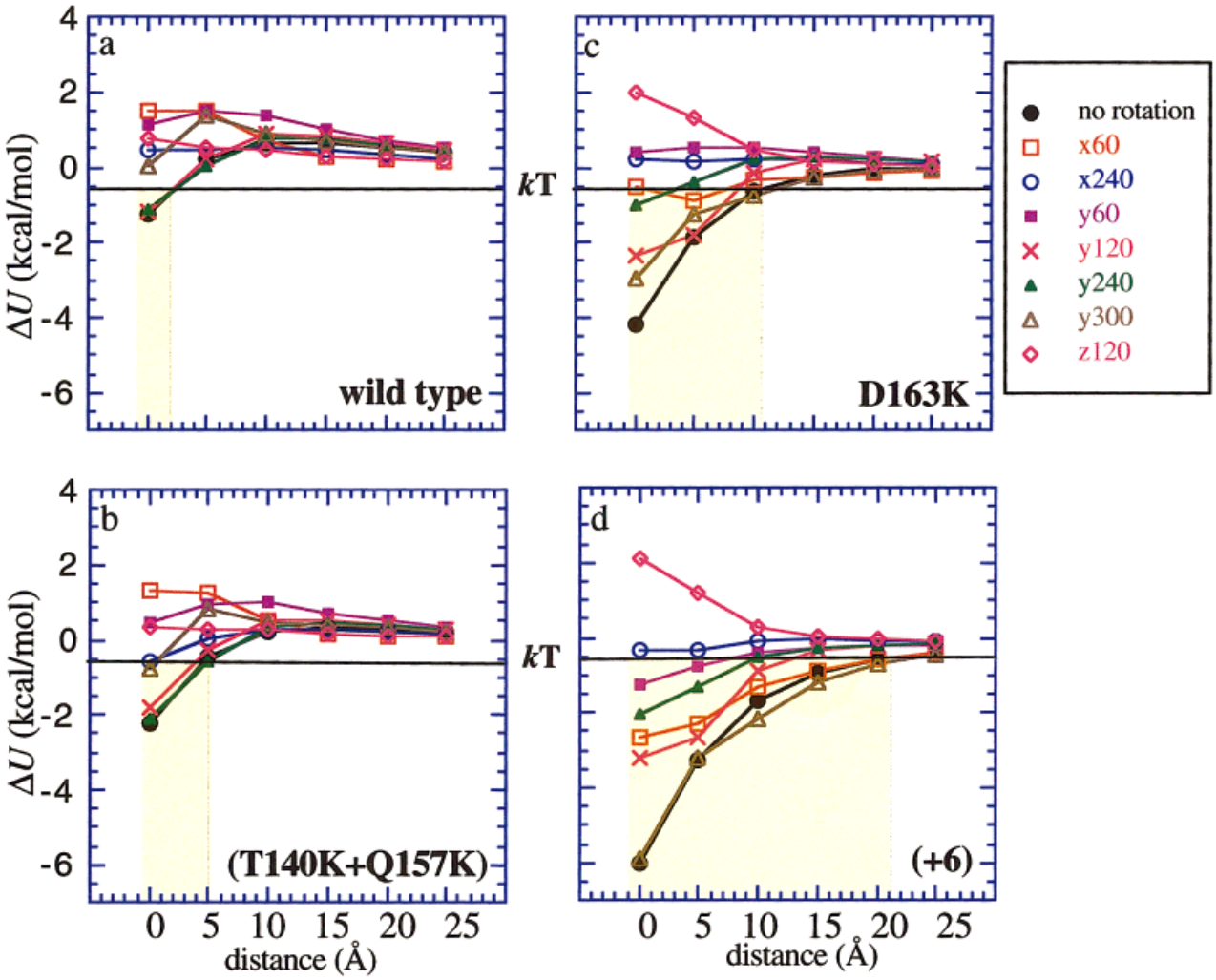

Fig. 3. Electrostatic energy of interaction of TEM1 with wt and mutated BLIP proteins as a function of the distance between them. Each line represents a different rotation of TEM1 along the indicated principal axis (see Fig. 2). **a– d:** are for wt and three Blip mutants. **a:** wt. **b:** (T140K + Q157K). **c:** D163K d: (+6) mutant (V165K + D163K + D135K + N89K). The steering region is represented by the shaded area, whose outer boundary is the distance where the electrostatic energy between the proteins is equal to RT = 0.59 kcal/mol (solid horizontal line).

opinion more accurately the pathway of association of TEM1 with BLIP. Moreover, we suggest that this is a general mechanism for protein–protein association.

The first step in protein–protein association is the formation of an encounter complex from the separated proteins. This step can be divided in two. Initially, the free proteins diffuse randomly in solution until they enter one into the electrostatic field of the other, here termed the *steering region*. Once entering the steering region, they move by directional diffusion toward the encounter complex. For the purpose of this discussion, we set the outer boundary of the steering region as a distance where $\Delta U = RT$. We have shown that the larger the electrostatic attraction between the proteins, the larger the volume of the steering region (Figs. 3–5). Hence, the proteins enter the steering region at an earlier stage along the reaction pathway, shortening the random diffusion step on account of increasing directional diffusion [see also Fig. 6(a)]. This can also be viewed as increasing the effective radii of the interacting proteins. Moreover, favorable electrostatic forces increase the attraction within the energy funnel as seen from the relative depth of the wells. Therefore, a larger proportion of the proteins within the steering region will form an encounter complex. Altogether, the net result of increasing ΔU is a faster k_1.

Once an encounter complex is formed, it can either evolve into the final complex (with a rate of k_2) or dissociate (with a rate of k_{-1}). The transition from the encounter complex to the final complex is classically viewed as being fast and not rate-limiting.[16,17,25] Therefore, Brownian dynamic simulations are often terminated as the proteins reach the encounter complex.[9] This would imply an energy diagram as shown in Figure 6(b), where the highest energy barrier is on the path of formation of the encounter complex. In this study, we reevaluate this assumption in light of the experimental observation that charge mutations of BLIP, which enhanced k_{on} by a factor of up to 250-fold, had no effect on the dissociation rate of the

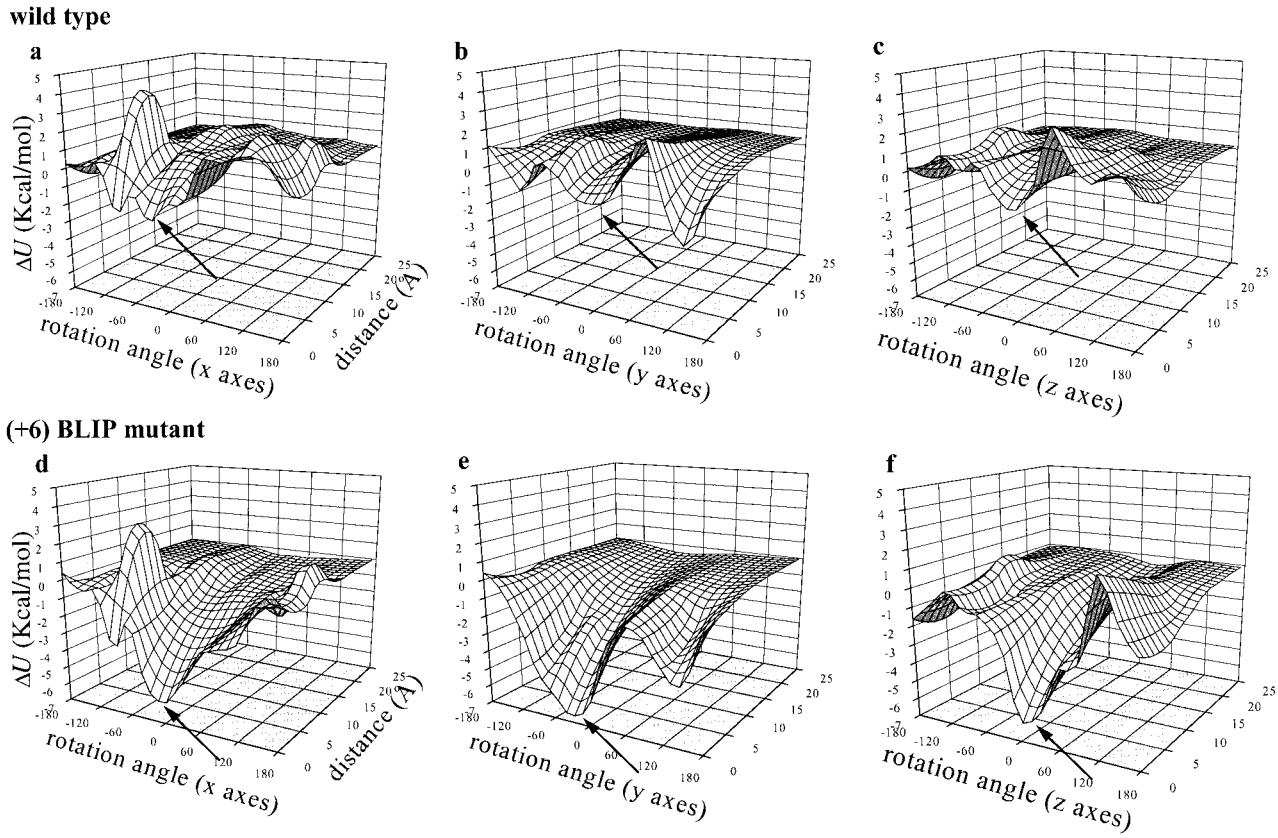

Fig. 4. Three-dimensional (3D) energy landscape of the association pathway of wt TEM1 with wt BLIP (**a–c**) and the (+6) BLIP mutant (**d–f**). The magnitude of the Debye–Hückel energy of interaction (ΔU) is plotted in 3D versus the distance and the relative rotation angle between the proteins. **a–c:** Association between TEM1 and wt BLIP, where TEM1 is rotated around its center of mass in the *y,z*-, *x,z*-, and *x,y*-planes respectively. **d–f:** Association between TEM1 and (+6) mutant of BLIP, where TEM1 is rotated around its center of mass in the *y,z*-, *x,z*-, and *x,y*-planes, respectively. The arrows point at the 0° rotation angle, which is the x-ray crystallographic structure of the TEM1–BLIP complex.

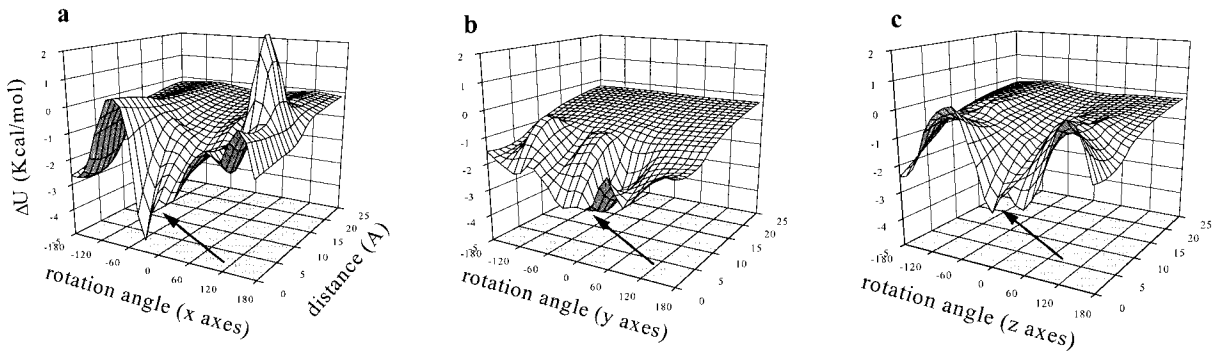

Fig. 5. Three-dimensional (3D) energy landscape of the association pathway of wt barnase and barstar. Starting with the final complex barnase was translated along the *y*-axes in 5 Å increments to a maximum distance of 25 Å. At each incremental distance, barnase was fixed, while barstar was rotated around its center of mass. Rotation was made around the three principal axes (see Figs. 2 and 4) with increments of 30°. **a–c:** Results of association with barstar rotating around its center of mass in the *y,z*-, *x,z*-, and *x,y*-plans, respectively. The arrows point on the 0° rotation angle, which is the x-ray crystallographic structure of the barnase–barstar complex.

protein complex, k_{off}.[14] Moreover, values of k_{off} were found to be independent of the salt concentration of the solution, clearly indicating that long-range electrostatic interactions play no significant role in the dissociation process. This fits our earlier observation that the Bronsted beta factor, measuring the relation between the activated complex and the final complex is close to one, indicating that they are both influenced by the same extend by long-range electrostatic forces.

In a two-step reaction mechanism in which the encounter complex is in steady state, k_{off} equals

$$k_{off} = \frac{k_{-1}k_{-2}}{k_{-1} + k_2} \quad (1)$$

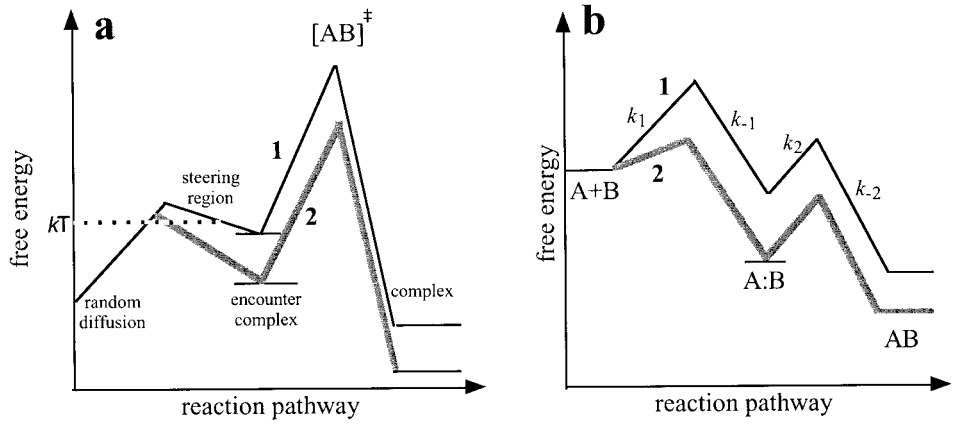

Fig. 6. Free energy profiles describing two possible pathways for protein–protein association. *A* + *B* represent the free proteins, *A:B* is the encounter complex, and AB is the final complex. **a:** Transition between the encounter complex and the final complex is the rate-limiting step for association. **b:** By contrast, the formation of the encounter complex is the rate-limiting step for association. Lines 1 and 2 describe the interaction between a pair of proteins in the absence and in the presence of favorable electrostatic forces.

Assuming that Figure 6(a) is correct, k_{-2} is independent of ΔU, while k_{-1} is expected to become slower with increasing ΔU [as k_{-1} represents the movement of the proteins against an electrostatic field which is increasing for faster associating mutant proteins (see Figs. 3 and 4)]. As k_{off} is not dependent on the magnitude of long-range electrostatic attraction, we have to assume that k_{-1} is not rate-limiting during protein–protein dissociation. Therefore, $k_{-1} \gg k_2$ leading to the relation $k_{off} = k_{-2}$. Thus, breaking the specific short-range interaction between the two proteins (k_{-2}) is the rate-limiting step for dissociation, whereas the rate at which the two proteins diffuse away from each other (k_{-1}) does not affect the overall dissociation rate constant k_{off}.

A different description of the association pathway is given in Figure 6(b). Here the major transition state is before the formation of [*A*:*B*]. Knowing that k_{off} is constant upon changing ΔU, both k_{-2} and k_{-1} have to be constant as well (see eq 1). As ΔU was shown to change dramatically with the distance between the proteins and their relative orientation (Fig. 4), this would suggest that the transition state between [A:B] and [A + B] is similar in structure to the encounter complex. Although this is theoretically possible, one has to ask: what is the nature of this transition state? The short-range interactions brake with a rate of k_{-2}. This transition occurs over a restricted volume of space, as the short-range interactions are cooperative and stereospecific. k_{-1} is the rate at which the encounter complex dissociates. This movement is driven by the entropy of moving from a pseudo-ordered encounter complex toward the unbound proteins and is slowed by the electrostatic forces that drive complex formation. As was shown, the entropic factor at this stage is small,[23] while the electrostatic forces can be significant and are mutant dependent. However, these electrostatic forces are additive, not stereospecific, and fade slowly over distance. Therefore, the transition state between [*A*:*B*] to [*A* + *B*] can be assumed to be relatively flat, and not restricted to the volume of space of the encounter complex. Accordingly, k_{-1} will decrease with increasing ΔU. But as k_{off} is constant,[14] this would contradict the experimental evidence, undermining the mechanism presented in Figure 6(b). The forthcoming discussion is based on the mechanism presented in Figure 6(a).

From Figure 6(a), the association rate constant is given by

$$k_{on} = \frac{k_1 k_2}{k_{-1} + k_2} = \frac{k_1 k_2}{k_{-1}} \qquad (2)$$

Accordingly, an increase in k_{on} can be a function of a faster k_1 or k_2, a slower k_{-1}, or a combination of these. It was previously shown for several protein-systems that the basal association rate (which is the rate of association in the absence of long-range steering forces) was unchanged upon changing the electrostatic attraction between the interacting proteins. Therefore, it will be reasonable to assume that the final docking step (k_2) is not highly influenced by mutation, even when charged residues are deleted from within the binding site. Moreover, the contribution of these changes to the rate of association is basically Coulombic in nature (as it can be calculated using PARE). This indicates that the net contribution of electrostatic interactions towards k_2 might be balanced by their unfavorable desolvation, which opposes binding. To summarize this part, the ratio of k_1/k_{-1} reflects the net association rate increase; however, moderate changes in k_2 cannot be excluded.

One may argue that in the case that $k_{-1} \gg k_2$ the binding process is reaction controlled, while it is well established that association (k_{on}) is diffusion controlled. Therefore, k_{-1} should not play an important role in determining k_{on}. However, this argument is flawed, as rates of association between TEM1 and BLIP were determined in low protein concentrations where the occupancy of the encounter complex is very small. Therefore, the result of lowering k_{-1} will be an increase in the occupancy of the encounter complex which will

cause a larger proportion of the proteins to evolve toward the final complex. A reaction controlled process will occur only when the encounter complex is highly populated, which will be achieved in the case of TEM1–BLIP at higher protein concentrations (similar to measurements of V_{max} in enzymatic reactions). For the association reaction of Ras with Raf, transient kinetic studies showed that the final docking step (k_2) occurs at a rate of several hundred per second.[26]

A question that emerges is why the two proteins in the encounter complex do not evolve rapidly to form the final complex. We attribute this to the weak electrostatic forces stabilizing the encounter complex, and the relative complexity of moving from the encounter complex toward the final complex. Several experimental studies support this notion. Activation free energies measured for 48 pairs of residues on barnase and barstar have revealed that only pairs of charged residues that are in close proximity in the final complex interact at the activated complex. The resulting coupling energies in the activated complex were only $\leq$0.5 kcal mol^{-1}, compared with up to 6.5 kcal mol^{-1} in the complex.[19] Furthermore at increased salt concentrations (masking electrostatic attraction) values of activation free energies were further reduced.[23] Thus, only specific, albeit weak electrostatic interactions are formed in the activated complex, and therefore at the encounter complex. Therefore, in the case that a high-energy barrier separates the encounter complex and the final complex, it is reasonable to assume that the encounter complex will dissociate more readily than it evolves to the final complex. This high-energy barrier can result from the need for structural rearrangement of the binding site and the precise structural alignment between the proteins before final docking. In contrast with protein folding (where the protein is flexible), in protein–protein association the two proteins have a rigid structure, making the process of structural rearrangement, and mutual alignment slow. Another possible reason for the high-energy barrier between the encounter complex and the final complex might be the energy cost of desolvation, energy cost of desolvation, especially of charged residues, which desolvation is thermodynamically very unfavorable.[11,27-29] Thus, electrostatic interactions, which are favorable at intermediate protein-protein separation distances, are unfavorable during final complex formation. The location of all charge mutation on BLIP outside the binding site, gives them a net favorable contribution to binding.

Characterization of Hotspots

An interesting outcome of the rational design project creating faster associating TEM1 and BLIP complexes was the notion that some residues are hotspot residues for association. This is also clearly seen in Figure 1. Some of the charge mutations cause a large shift in k_{on} (>10-fold), while others do not. The simulation presented in Figure 3 provides an interesting insight regarding the nature of hotspot residues for association. Two BLIP variants whose net charges were changed by +2 are presented in Figure 3(b) and 3(c) . Whereas D163K increases k_{on} by 23-fold, the BLIP (T140K + Q157K) variant increases k_{on} by only 5-fold (relative to wt). The steering region guiding the D163K mutant extends for a longer distance, with the energy funnel being deeper compared with the BLIP (T140K + Q157K) mutant (Fig. 3). Thus, a hotspot residue appears to be located at a site where the charge confers a maximal efficiency toward steering the two proteins together. Hence, the rate of association is not directly related to the overall charge in the vicinity of the binding site, but rather to the specific distribution of charges. For example, in the TEM1–BLIP complex, the residues on TEM1 located close to BLIP D163 are E104, E168, and E171 (distance between charges 5–7 Å[30]), and R164 and E166 located 8 and 9 Å from D163.[30] Thus, residue 163 on BLIP "feels" a strong, specific electrostatic field generated from the negatively charged patch on TEM1. Therefore mutating D163 to a base relieves the local electrostatic repulsion and adds favorable attraction. On the other hand, neither T140 nor Q157 on BLIP is located in the vicinity of a charged patch on TEM1, so introducing a base instead of these two residues has a limited effect on association.

Hotspots for association are found naturally in proteins. An extreme case is the 250-fold reduction in k_{on} upon mutation of Lys 15 on BPTI to Ala in its interaction with trypsin, despite the fact that both proteins have a net charge of the same positive sign.[31] Another example are the mutations R144A or K133A in IFNa2 which cause a reduction of 10- and 5-fold in k_{on} with ifnar2, while all other mutations cause changes in rates of <2-fold.[32] On barnase, K27 and R59 have double the contribution toward k_{on} than all other mutations analyzed.[21] Thus, it appears that hotspots for association can either be found, or engineered into many protein systems. All hotspots analyzed so far are located within or at the vicinity of the binding site, and are fully exposed residues on the protein surface not buried in pockets or grooves. The existence of hotspots for association also indicates that stabilization of an encounter complex which resembles in structure the final complex is important in increasing the rate of association.

Application of PARE for Molecular Docking

An interesting outcome of our simulations is that PARE can be used for protein docking, in cases in which the docked structure of the complex is unknown. The basic idea is to correlate between association rates of different mutant complexes as determined experimentally and the theoretically calculated values using a modeled structure. The quality of the correlation serves as a tool for evaluating the quality of the final docked structure of a protein complex. Figure 7 shows the correlation between the experimental and calculated rates of association of TEM1 with wt and mutant BLIP proteins. Each line stands for a PARE calculation performed for all BLIP mutants available, albeit at different relative orientations representing different artificial docking conformations. Each point along the line stands

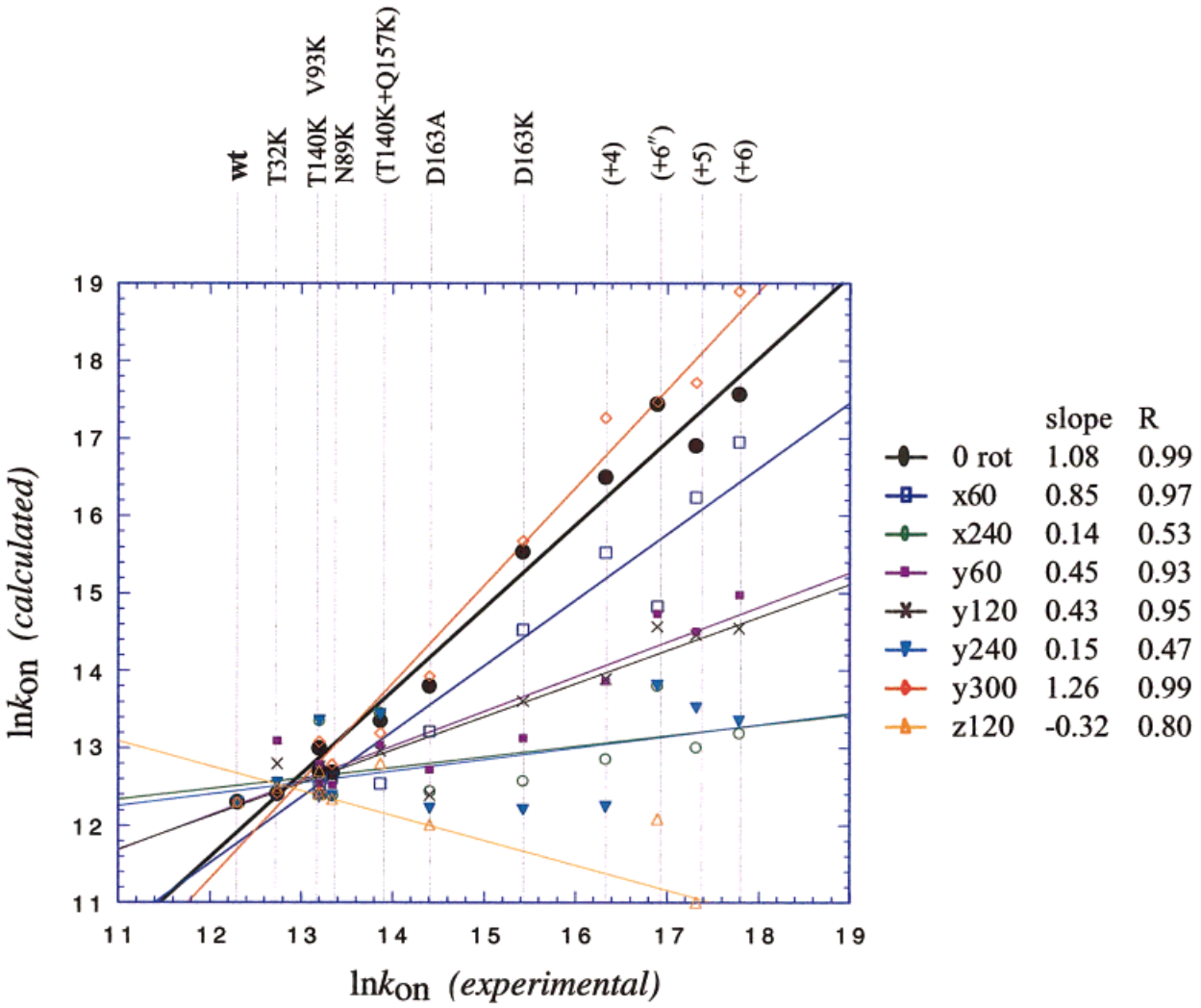

Fig. 7. Validating PARE as a tool for protein docking. Graphic representation of the correlation between the experimentally determined association rates of different TEM1–BLIP mutant complexes and the theoretically calculated values. Each line stands for a set of calculations performed for different BLIP mutants at different artificial docking conformation. Each point along the line represents a different BLIP mutant. Values of the slopes and correlation coefficient for each docking conformation are given in the table on the right. Calculations of lnk_{on} (at I = 0.022 M) were performed using the program PARE.[14] Experimental values of ln k_{on} (at I = 0.022 M) are from Selzer et al.[14] (+6) = (V165K + D163K + D135K + N89K); (+6″) = (V165K + D163K + Q157K + T140K + A77K); (+5) = (D163K + D135K + V134K); (+4) = (V165K + D163K + N89K).

for a different BLIP mutant. The experimental values of k_{on} in Figure 7 are a measure of the rate of formation of the correct orientation, whereas the theoretically calculated values of k_{on} represent the calculated rate for the different orientations. In evaluating the linear fits between experimental and calculated values, attention should be paid to two parameters: The slope of the linear fit, which should be close or equal to 1, and the correlation coefficient of the linear fit, which should reach the value of 1. As can be seen in Figure 7, both parameters are best satisfied when the simulation uses the x-ray crystallographic structure of the TEM1–BLIP complex (represented by the thickest line). Although the linear fit with the x- or y-axes should theoretically pass through the origin of the coordination system, the exact value of the intercept in this case is less important, as it is negligible relative to the k_{on} values ($>10^5$ $M^{-1}s^{-1}$). This docking strategy may not be sufficient by itself to determine the precise structure of the complex, although it seems to be a powerful tool to distinguish between possible true and false conformations, in the sense that they appear to have highly unfavorable electrostatic contributions to binding.

In this work, we have combined experimental data with theoretical calculations to decipher the pathway of protein association. A general two step mechanism for association has been described, where the rate-limiting step for association is the formation of the final complex from the encounter complex. Increasing specific long-range electrostatic forces result in a faster k_1 and a slower k_{-1}, with the ratio between them giving the rate increase. The existence of hotspot residues for association was discussed, and the applicability of calculating rates of association for protein docking was demonstrated.

ACKNOWLEDGMENTS

G.S. is incumbent of the Dewey David Stone and Harry Levine career development chair. This research was supported by a research grant from the Crown endowment fund for immunological research. We thank Shira Albeck for her critical reading of the manuscript.

REFERENCES

1. Smoluchowski MV. Versuch einer mathematischen Theorie der Koagulationskinetik kolloider Lösungen. Z Phys Chem 1918;92: 129.
2. Berg OG, von Hippel PH. Diffusion-controlled macromolecular interactions. Annu Rev Biophys Chem 1985;14:131–160.
3. Northrup SH, Erickson HP. Kinetics of protein–protein association explained by Brownian dynamic computer simulation. Proc Natl Acad Sci USA 1992;89:3338–3342.
4. Camacho CJ, Weng Z, Vajda S, DeLisi C. Free energy landscapes of encounter complexes in protein–protein association. Biophys J 1999;76:1166–1178.
5. Getzoff ED, Cabelli DE, Fisher CL, Parge HE, Viezzoli MS, Banci L, Hallewell RA. Faster superoxide dismutase mutants designed by enhancing electrostatic guidance. Nature 1992; 358:347–351.
6. Kozack UE, d'Mello MJ, Subramanian S. Computer modeling of electrostatic steering and orientational effects in antibody–antigen association. Biophys J 1995; 68:807–814.
7. Madura JD, Briggs JM, Wade RC, Davis ME, Luty BA, Ilin A, Antosiewicz J, Gilson MK, Gagheri B, Scott LR, McCammon JA. Electrostatic and diffusion of molecules in solution: Simulations with the University of Houston Brownian Dynamics Program. Comput Phys Commun 1995;91:57–95.
8. Gabdoulline RR, Wade RC. Simulation of the diffusional association of barnase and barstar. Biophys J 1997;72:1917–1929.
9. Gabdoulline RR, Wade RC. Brownian dynamics simulation of protein–protein diffusional encounter. Methods 1998;14:329–341.
10. Davis ME, Madura JD, Luty BA, McCammon JA. Electrostatics and diffusion of molecules in solution: Simulations with the University of Houston Brownian dynamics program. Comput Phys Commun 1991;62:187–197.
11. Elcock AH, Gabdoulline RR, Wade RC, McCammon JA. Computer simulation of protein–protein association kinetics: Acetylcholinesterase–fasciculin. J Mol Biol 1999;291:149–162.
12. Zhou HX, Wong KY, Vijayakumar M. Design of fast enzymes by optimizing interaction potential in active site. Proc Natl Acad Sci USA 1997;94:12372–12377.
13. Vijayakumar M, Wong KY, Schreiber G, Fersht AR, Szabo A, Zhou HZ. Electrostatic enhancement of diffusion-controlled protein–protein association: Comparison of theory and experiment on barnase and barstar. J Mol Biol 1998;278:1015–1024.
14. Selzer T, Albeck S, Schreiber G. Rational design of faster associating and tighter binding protein complexes. Nature Struct Biol 2000;7:537–541.
15. Camacho CJ, Kimura SR, DeLisi C, Vajda S. Kinetics of desolvation-mediated protein–protein binding. Biophys J 2000;78:1094–1105.
16. Gabdoulline RR, Wade RC. On the protein–protein diffusional encounter complex. J Mol Recognit 1999;12:226–234.
17. Janin J. The kinetics of protein–protein recognition. Proteins 1997;28:153–161.
18. von Hippel PH, Berg OG. Facilitated target location in biological systems. J Biol Chem 1989;264:675–678.
19. Schreiber G, Fersht AR. Rapid, electrostatic assisted, association of proteins. Nature Struct Biol 1996;3:427–431.
20. Selzer T, Schreiber G. Predicting the rate enhancement of protein complex formation from the electrostatic energy of interaction. J Mol Biol 1999;287:409–419.
21. Schreiber G, Fersht AR. Energetics of protein–protein interactions: Analysis of the barnase–barstar interface by single mutations and double mutant cycles. J Mol Biol 1995;248:478–486.
22. Albeck S, Schreiber G. Biophysical characterization of the interaction of the β-lactamase TEM-1 with its protein inhibitor BLIP. Biochemistry 1999;38:11–21.
23. Frisch C, Fersht AR, Schreiber G. Experimental assignment of the structure of the transition state for the association of barnase and barstar. J Mol Biol 2001;308:69–77.
24. Schreiber G, Frisch C, Fersht AR. The role of Glu73 of barnase in catalysis and the binding of barstar. J Mol Biol 1997;270:111–122.
25. Taylor MG, Rajpal A, Kirsch JF. Kinetic epitope mapping of the chicken lysozyme HyHel-10 Fab complex: Delineation of docking trajectories. Protein Sci 1998;7:1857–1867.
26. Sydor JR, Engelhard M, Wittinghofer A, Goody RS, Herrmann C. Transient kinetic studies on the interaction of Ras and the Ras-binding domain of c-Raf-1 reveal rapid equilibration of the complex. Biochemistry 1998;37:14292–14299.
27. Hendsch ZS, Tidor B. Do salt bridges stabilize proteins? A continuum electrostatic analysis. Protein Sci 1994;3:211–226.
28. Sheinerman FB, Norel R, Honig B. Electrostatic aspects or protein-protein interactions. Curr Opin Struct Biol 2000;10:153–159.
29. Albeck S, Unger R, Schreiber G. Evaluation of direct and cooperative contributions toward the strength of buried hydrogen bonds and salt bridges. J Mol Biol 2000;298:503–520.
30. Strynadka NCJ, Jensen SE, Alzari PM, James MNGA. Potent new mode of β-lactamase inhibition revealed by the 1.7 Å X-ray crystallographic structure of the TEM-1–BLIP complex. Nature Struct Biol 1996;3:290–297.
31. Castro MJ, Anderson S. Alanine point-mutations in the reactive region of bovine pancreatic trypsin inhibitor: Effects on the kinetics and thermodynamics of binding to β-trypsin and α-chymotrypsin. Biochemistry 1996;35:11435–11446.
32. Piehler J, Schreiber G. Mutational and structural analysis of the binding interface between type I interferons and their receptor ifnar2. J Mol Biol 1999;294:223–237.
33. Collaborative Computational Project, N. The CCP4 suite: Programs for protein crystallography. Acta Crystallogr D Biol Crystallogr 1994;50:760–763.